International Journal of ChemTech Research
CODEN (USA): IJCRGG ISSN: 0974-4290
Vol.8, No.1, pp 228-240, 2015

Synthesis, Crystal Structure and Antimicrobial Properties of N-(4-chlorobenzyl)piperazinium Tetrachlorocuprate(II)

N. Dhanam[1]* and A. Thamaraichelvan[2]

[1]D.K.M. College for women (Autonomous), Vellore-632 001, Tamilnadu, India
[2]Thiagarajar College, Madurai-625 009, Tamilnadu, India

Abstract: The synthesis and crystal structure of the title compound, [N-(4 chlorobenzyl) piperazineH_2]$CuCl_4$.Cl_2 of molecular formula $C_{22}H_{34}N_4Cl_2CuCl_6$ has been prepared and studied by X-ray diffraction method. The crystals are orthorhombic, Abm_2, with a = 7.1344(2), b = 44.191(2), c = 9.1061(4), z = 4 and a final R value of 0.0289. Flattening of the tetrahedral $CuCl_4^{2-}$ anion occurs to such an extent that the structure is closer to the rarely encountered slightly distorted square with an average trans angle of 166.305°. The structure consists of a $CuCl_4^{2-}$ anion, two lattice Cl^- ions and two $(N\text{-}4\text{-}ClBzPipzH_2)^{2+}$cation which are hydrogen bonded to anions through N-H…..Cl weak bonds thus stabilizing the planar like geometry of the anion. The electronic spectrum reveals the d-d and charge transfer bands at 450 nm and 320 nm respectively. The protonation of N-(4-chlorobenzyl)piperazine moiety and the occurrence of hydrogen bonding interactions are deduced from vibrational spectra. The thermal analysis is in accordance with the structural features. Computational studies established the presence of H-bonding and other interactions among the various moieties. Further, anti-microbial activities of the compound have also been established.
Key words: Chlorocuprates(II), N-(4-chlorobenzyl)piperazine, XRD, H-bonding, DFT-studies.

Introduction

Piperazine derivatives have been extensively investigated due to their biological activities. They have a wide range of clinical applications in the therapy of functional diseases and exhibit anthelmintic, antibacterial and insecticidal activities [1] and many important pharmacological properties.

The importance of salts of nitrogen heterocyclics with transition metal halides has been ever growing due to interesting packing structures [2, 3, 4], solid-state reactions [5], optical [6], magnetic [7] and redox properties [8], structures that make them model compounds for biological processes [9], electronic [10] and opto electronic properties [11]. The hybrid organo-ammonium halometallate(II) has been exploited as a semiconducting material [12]. Catalytic ionic liquids are synthesized using ionic liquids and chlorometallate ions. Such compounds possess a catalytically active cation or anion or both [13].

Interest in tetrachlorocuprates(II) arises due to a variety of interesting stereochemical features like pseudotetrahedral with D_{2d} symmetry [14], planar and pyramidal geometry [15]. In general, the size of the cation strongly influences the structure of the tetracholocuprate(II) anion. Bulky organic cations force the anions to exist as dimers or discrete monomers with strictly four-coordinated copper(II) [16]. The geometry of the $[CuCl_4]^{2-}$ anion depends on many factors, including the Jahn-Teller effect, electrostatic repulsion between Cl atoms, crystal packing forces and hydrogen bonding [17]. Their reactivity depends mainly on the two factors viz., the number of halide anions in the coordination sphere and the nuclearity [18]. While J-T effect lowers the

symmetry of Cu(II) below tetragonal [19], square planar geometry appears to be the extreme case strongly stabilized by hydrogen bonding to the organic cations and crystal packing forces [20].

In view of the interesting structural variations observed in tetrachlorocuprates(II) influenced by the size and hydrogen bonding nature of the organic cations, we report here the synthesis, crystal structure and characterization by thermal, spectral, computational, electrochemical and antimicrobial activity studies of N-(4-chlorobenzyl)piperazinium tetrachlorocuprate(II) for the first time. N-(4-chlorobenzyl)piperazine was deliberately chosen as the organic moiety since it forms a bulky cation to counter balance the $CuCl_4^{2-}$ anions.

Experimental

Materials and methods

N-(4-chlorobenzyl)piperazine and $CuCl_2.2H_2O$ were used as purchased (Merck). The hydrochloric acid was of reagent grade and used without further purification. The elements C, H and N were determined using a CHNS analyzer, Varian Micro cube and LECO CHNS-932. Thermogravimetric and Differential Thermal analysis were carried out using NETZSCH STA 409/C/CD instrument in the range of 20-700˚C with platinum crucible in the presence of nitrogen and a scanning rate of 10.0˚C min^{-1}. FT-IR spectral measurements were made in a JASCO FT-IR 460 plus Spectrophotometer using KBr pellets in the range of 4000-400 cm^{-1}. A JASCO 530V UV-Visible spectrophotometer was employed to record the electronic spectra in the range of 200-1000 nm with a quartz cell of 1 cm path length. Acetonitrile was used as reference solvent for all measurement.

Crystal Structure determination

Table 1. Crystal data and structure refinement parameters

Crystal data	**Shelxl data [**CCDC 882861]
Empirical formula	C_{22} H_{34} Cl_8 Cu N_4
Formula weight	701.67
Temperature (K)	293(2)
Crystal system, space group	orthorhombic, Abm2
Unit cell constants: a (Å) b (Å) c (Å)	7.1344(2) 44.191(2) 9.1061(4)
β(^{0})	90.00
Volume ($A^{\circ 3}$)	2870.9(2)
Z, D (calculated) (Mg m^{-3})	4
Crystal size(mm)	0.30X 0.20 X 0.20
F(000)	1436
Crystal form , colour	green
θ range(^{o}) for data collection	2.5-25.6
No. of reflections collected	2537
Data collection method	'\w and \f scan'
T min and T max	0.610 and 0.723
Range of h, k, l	-5-8 , -52-52, -10 - 10
No. of parameters	167
Goodness – of- fit on F^2	1.032
Final R indices[I> 2 σ (F^2)], w$R(F^2)$, S	0.0737 0.0724
R indices (all data) R1, w$R(F^2)$	0.0289, 0.0272
$\Delta\rho_{max}$, Δ ρ_{min}(e $Å^{-3}$)	1.62 -0.778

The green coloured crystal having approximate dimensions of 0.30 mm x 0.20 mm x 0.2 mm was mounted on a glass fiber for structure determination. The data collection was performed in a Nonius MACH3 diffractometer with ω-2θ scans. All measurements were made with graphite monochromated MoKα radiation.

A total of 2537 reflections were obtained with θ ranging from 2.5°-25.6°. Cell parameters and an orientation matrix for data collection were obtained from least squares analysis using SHELXL-97. The structure was solved using Fourier Techniques. The non-hydrogen atoms were refined anisotropically. Hydrogen atom positions were calculated using a riding model and were refined isotropically. The final R value was 0.0289. The crystal structure was solved using SHELXS and SHELXL programs [21]. The crystal data and the refinement parameters are presented in table 2.

Table 2. Experimental and theoretical bond lengths (A°)

Experimental			Theoretical		
Atom1	**Atom2**	**Length**	**Atom1**	**Atom2**	**Length**
`C1	C2	1.378(5)	C1	C2	1.3907
C1	C6	1.377(5)	C1	C9	1.3925
C1	Cl1	1.732(4)	C1	Cl30	1.7540
C2	H2	0.930(4)	C2	H3	1.0830
C2	C3	1.381(5)	C2	C4	1.3918
C3	H3	0.930(3)	C4	H5	1.0861
C3	C4	1.387(4)	C4	C6	1.3979
C4	C5	1.397(4)	C6	C7	1.4008
C4	C7	1.504(4)	C6	C11	1.5072
C5	H5	0.930(4)	C7	H8	1.0856
C5	C6	1.386(5)	C7	C9	1.3906
C6	H6	0.931(4)	C9	H10	1.0829
C7	H7A	0.970(3)	C11	H12	1.0923
C7	H7B	0.970(3)	C11	H13	1.0920
C7	N1	1.505(4)	C11	N26	1.5115
C8	H8A	0.969(3)	C14	H15	1.0881
C8	H8B	0.970(3)	C14	H16	1.0933
C8	C9	1.515(4)	C14	C17	1.5208
C8	N1	1.486(4)	C14	N26	1.4976
C9	H9A	0.970(3)	C17	H18	1.0905
C9	H9B	0.970(3)	C17	H19	1.0906
C9	N2	1.485(4)	C17	N27	1.4961
C10	H10A	0.970(3)	C20	H21	1.0903
C10	H10B	0.969(3)	C20	H22	1.0901
C10	C11	1.511(4)	C20	C23	1.5237
C10	N2	1.486(4)	C20	N27	1.4915
C11	H11A	0.969(3)	C23	H24	1.0930
C11	H11B	0.970(3)	C23	H25	1.0900
C11	N1	1.496(4)	C23	N26	1.4989
N1	H1	0.94(4)	N26	H31	1.1056
N2	H2A	0.901(2)	N27	H28	1.0467
N2	H2B	0.901(2)	N27	H29	1.0352
Cl3	Cu1	2.2461(6)	Cl32	Cu35	2.3087
Cl4	Cu1	2.261(2)	Cl33	Cu35	2.4254
Cl5	Cu1	2.321(1)	Cl34	Cu35	2.3115
Cu1	Cl3	2.2461(6)	Cu35	Cl36	2.4231

Computational methods

DFT calculations were performed for the titled crystal. The primary geometry from the crystal structure coordinates was optimized without restraint in the Beeke's three parameter exchange functional with Lee-Yang-Parr gradient corrected correlation functional(B3LYP) [22, 23] in conjunction with the Loss Alamos ECP plus Double Zeta Basis sets(LanL2DZ) [24], using HP Proliant DL160 G5 servers with Quad-core Intel Xeon processors by employing Gaussian 03W program package. The molecular geometry of the complex was fully optimized into the global minima. The optimized structural parameters were used for the vibrational frequency calculations at the DFT level to analyze all stationary points as minima.

Antibacterial assay

Muller Hilton Agar was prepared and sterilized. 20 mL of media was poured in petriplates and allowed for solidification. The bacterial lawn cultures of *Staphylococcus aureus* and *Escherichia coli* were made using sterile cotton swab and labeled. The wells were made in the media with the help of a metallic borer with at least 24 mm in diameter. Recommended concentration of 50 µL of the test sample (10 mg/mL in DMSO) was introduced in the respective wells. The plates were incubated immediately at 37 ℃ for 24 hours. Activity was determined by measuring the diameter of zones showing complete inhibition (mm). Growth inhibition was compared with that by the standard drug [25].

Antifungal assay

The antifungal activity was studied against two fungal cultures of *Colletotrichum* and *Fusarium* species. Sabouraud dextrose agar was prepared, sterilized and the culture plates were prepared in a similar way as that used for Muller Hilton Agar. After solidification of the media, respective fungal spore suspensions were transferred to petri plates. The wells were made in the media with the help of a sterile metallic borer with at least 24 mm in diameter. Concentration of 50 μL of the test sample (10 mg/mL) in DMSO was introduced in the wells. The plates were incubated at 30°C for 72 hours. The results were recorded as zones of inhibition in mm [26]. The experiments were repeated for 100 μL concentration.

Synthesis

An 10 mL aqueous solution containing $CuCl_2.2H_2O$ (1 mmol, 0.85g) and N-(4-chloro benzyl)piperazine (1 mmol, 1.05g) in 2 mL ethanol were mixed slowly, a dark green colored precipitate was obtained. The precipitate was dissolved by drop-wise addition of 1 mL of (12 N) concentrated hydrochloric acid in 10 mL of water via a Pasteur pipette to the mixture. The resulting clear solution was filtered off and kept undisturbed for crystallization. Pale green colored crystals were formed over a period of one week. The crystals were collected by filtration and washed with 95% ethanol and then diethyl ether, dried and preserved in a desiccator (94%). Anal.Found. for C_{22} H_{34} Cl_8 Cu N_4 (F.wt. 701.67) : C 25.91, H 3.95, N 16.06, Calc: C 25.88, H 3.91, N 16.07, μ_{eff} = 1.61.

Results and Discussion

The complex is green colored crystal and found to be stable at ambient temperature and is insoluble in common organic solvents but are soluble in coordinating solvents such as DMSO, DMF and acetonitrile. The conductivity measurement showed molar conductivity value of 133 Ω^{-1} cm^2 mol^{-1} in water representing the property of good electrolytic in nature [27].

The ORTEP diagram with atom labeling scheme is shown in figure 1. The structure consists of one discrete $CuCl_4^{2-}$ anion and two 4-chlorobenzylpiperazinium cations. The compound crystallizes in the orthorhombic space group of Abm_2.The asymmetric unit within the unit cell comprises of one $[CuCl_4]^{2-}$ anion, one $[N\text{-}(4\text{-}ClBzPipzH_2]^{2+}$ cation and a Cl^- ion as illustrated in figure 2.

Description of the Crystal Structure

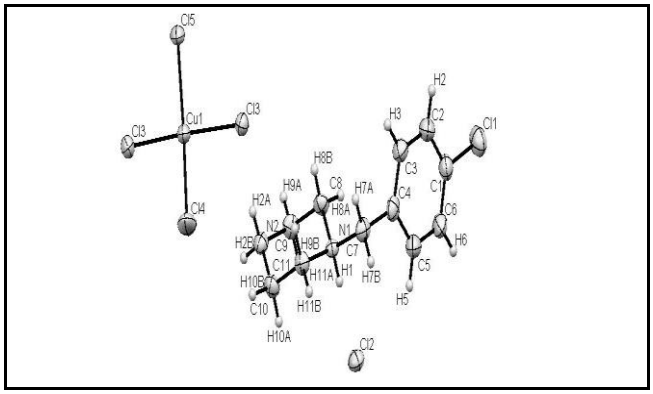

Fig 1. ORTEP diagram showing the atomic labeling scheme

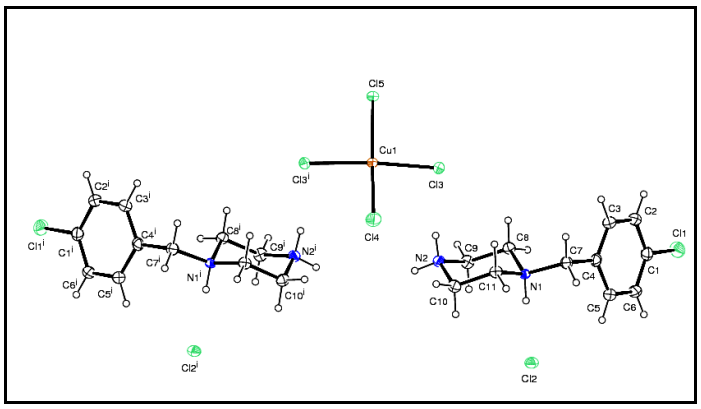

Fig 2. Asymmetric unit

Table 3. Experimental and theoretical bond angles (°)

Experimental				Theoretical			
Atom1	**Atom2**	**Atom3**	**Angle**	**Atom1**	**Atom2**	**Atom3**	**Angle**
C2	C1	C6	120.6(3)	C2	C1	C9	121.10
C2	C1	Cl1	119.8(3)	C2	C1	Cl30	119.41
C6	C1	Cl1	119.6(3)	C9	C1	Cl30	119.50
C1	C2	H2	120.2(3)	C1	C2	H3	120.29
C1	C2	C3	119.7(3)	C1	C2	C4	118.99
H2	C2	C3	120.1(3)	H3	C2	C4	120.73
C2	C3	H3	119.6(3)	C2	C4	H5	118.89
C2	C3	C4	120.9(3)	C2	C4	C6	120.96
H3	C3	C4	119.5(3)	H5	C4	C6	120.15
C3	C4	C5	118.7(3)	C4	C6	C7	119.07
C3	C4	C7	119.9(3)	C4	C6	C11	119.96
C5	C4	C7	121.4(3)	C7	C6	C11	120.95
C4	C5	H5	119.9(3)	C6	C7	H8	120.26
C4	C5	C6	120.4(3)	C6	C7	C9	120.43
H5	C5	C6	119.8(3)	H8	C7	C9	119.29
C1	C6	C5	119.8(3)	C1	C9	C7	119.45
C1	C6	H6	120.1(3)	C1	C9	H10	120.20
C5	C6	H6	120.1(3)	C7	C9	H10	120.35
C4	C7	H7A	109.0(3)	C6	C11	H12	110.78
C4	C7	H7B	109.0(3)	C6	C11	H13	111.01
C4	C7	N1	113.0(2)	C6	C11	N26	114.28
H7A	C7	H7B	107.8(3)	H12	C11	H13	108.27
H7A	C7	N1	109.0(2)	H12	C11	N26	107.24
H7B	C7	N1	108.9(2)	H13	C11	N26	104.91
H8A	C8	H8B	108.2(3)	H15	C14	H16	108.64
H8A	C8	C9	109.6(3)	H15	C14	C17	109.64
H8A	C8	N1	109.6(2)	H15	C14	N26	107.85
H8B	C8	C9	109.6(3)	H16	C14	C17	111.10
H8B	C8	N1	109.6(2)	H16	C14	N26	108.88
C9	C8	N1	110.2(2)	C17	C14	N26	110.64
C8	C9	H9A	109.4(3)	C14	C17	H18	109.70
C8	C9	H9B	109.5(3)	C14	C17	H19	111.45
C8	C9	N2	111.3(2)	C14	C17	N27	109.16
H9A	C9	H9B	108.0(3)	H18	C17	H19	110.66
H9A	C9	N2	109.3(3)	H18	C17	N27	107.59
H9B	C9	N2	109.3(3)	H19	C17	N27	108.17
H10A	C10	H10B	108.2(3)	H21	C20	H22	109.98
H10A	C10	C11	109.6(3)	H21	C20	C23	110.82

H10A	C10	N2	109.7(3)	H21	C20	N27	108.69
H10B	C10	C11	109.6(3)	H22	C20	C23	110.16
H10B	C10	N2	109.7(3)	H22	C20	N27	107.99
C11	C10	N2	110.0(2)	C23	C20	N27	109.13
C10	C11	H11A	109.5(3)	C20	C23	H24	111.37
C10	C11	H11B	109.4(3)	C20	C23	H25	109.17
C10	C11	N1	111.1(2)	C20	C23	N26	111.12
H11A	C11	H11B	108.0(3)	H24	C23	H25	109.21
H11A	C11	N1	109.4(2)	H24	C23	N26	108.47
H11B	C11	N1	109.4(2)	H25	C23	N26	107.40
C7	N1	C8	113.2(2)	C11	N26	C14	113.91
C7	N1	C11	110.3(2)	C11	N26	C23	110.52
C7	N1	H1	107(2)	C11	N26	H31	107.64
C8	N1	C11	109.1(2)	C14	N26	C23	111.47
C8	N1	H1	107(2)	C14	N26	H31	108.22
C11	N1	H1	110(2)	C23	N26	H31	104.54
C9	N2	C10	110.8(2)	C17	N27	C20	112.39
C9	N2	H2A	109.5(2)	C17	N27	H28	108.98
C9	N2	H2B	109.6(2)	C17	N27	H29	111.48
C10	N2	H2A	109.5(2)	C20	N27	H28	108.83
C10	N2	H2B	109.5(2)	C20	N27	H29	112.45
H2A	N2	H2B	108.0(2)	H28	N27	H29	102.15
Cl3	Cu1	Cl4	91.09(5)	Cl32	Cu35	Cl33	102.33
Cl3	Cu1	Cl5	90.51(4)	Cl32	Cu35	Cl34	143.36
Cl3	Cu1	Cl3	167.92(3)	Cl32	Cu35	Cl36	98.58
Cl4	Cu1	Cl5	164.69(5)	Cl33	Cu35	Cl34	98.70
Cl4	Cu1	Cl3	91.09(5)	Cl33	Cu35	Cl36	109.19
Cl5	Cu1	Cl3	90.51(4)	Cl34	Cu35	Cl36	102.39

Table 4. Hydrogen bonding data

D-H…A	d(D-H) (distance) A°	d(H…A) A°	d(D…A) A°	<(DHA) degrees
N(2)-H(2B)…C1(5)	0.90	2.24	3.129	169.8
N(2)-H(2A)…C1(3)	0.90	2.26	3.128(2)	161.9

Symmetry transformations used to generate equivalent atoms#1 –x+2, -y+1, -z #2 x, -y+3/2, z+1/2

The experimental and theoretical values for selected bond lengths and bond angles are provided in tables 3 and 4 respectively. The coordination geometry about the copper atom shows distortion of the tetrahedron super imposable on the basic square planar configuration since the Cl_3-Cu-Cl_4 and Cl_4-Cu-Cl_3 bond angles are 90.51(4) deg and 91.09(5) deg respectively with trans angle of 164.69° and 167.92°. Hence the geometry of $CuCl_4^{2-}$ may be regarded as distorted square. The bond angles and bond lengths are comparable to those observed for N-(1-benzyl)piperazinium tetrachlorocuprate(II), with monoclinic space group Pc (C_s^2. No. 7) in the crystalline state (θ = 166.4) [28]. The structure of $CuCl_4^{2-}$ anion corresponds to an unequally flattened tetrahedral leading to a limiting planar configuration.

A comparison of Cu-Cl bond lengths reveals that while the values are 2.234, 2.249, 2.252 and 2.334 for N-(1-benzyl)piperazinium tetrachlorocuprate(II), the corresponding values for **1** are 2.2461, 2.2461, 2.261 and 2.321. The average values of Cl-Cu-Cl bond angles and Cu-Cl bond lengths are 115.97° and 2.2685A° respectively. The values are comparable to 116° and 2.2672A° observed for the parent compound [28]. Since the chlorine at the 4th position of phenyl ring is not involved in H-bonding, its presence does not alter the bond lengths and bond angles to a greater degree. However it affects the space group.

The average bond distance for the C-N linkages in the present system is 1.4916Å which is comparable to 1.496Å reported for N-(1-benzyl)piperazinium tetrachlorocuprate(II) [28]. The elongation of bond is expected due to the N-H….Cl type of hydrogen bonding interactions involving the hydrogen atoms linked to nitrogen and

halide of anionic $CuCl_4^{2-}$ unit. The extensive hydrogen bonding network along c axis is shown in figure 3. The molecular packing of the crystal lattice, along a axis, could be seen in figure 4.

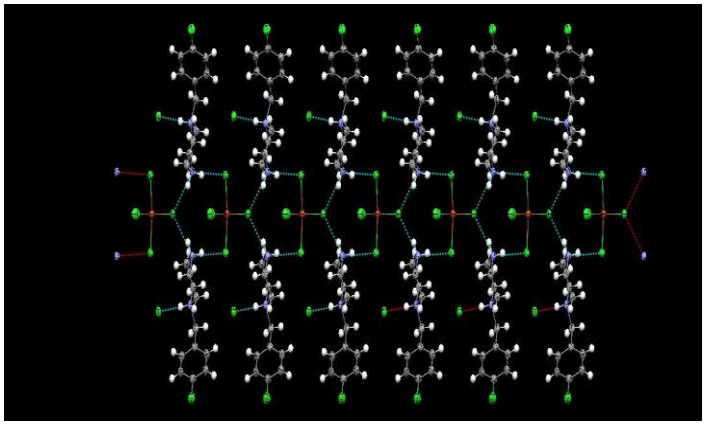

Fig 3. Hydrogen bonding network along c axis

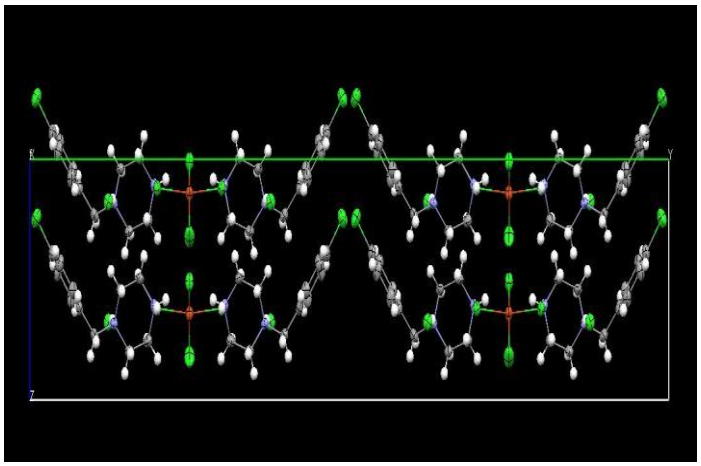

Fig 4. Molecular packing diagram along a axis

Although the geometry of $CuCl_4^{2-}$ anion is similar to that of N-benzylpiperazinium tetrachlorocuprate (II), the crystal system and **s**pace group are significantly different (table 1). This may be due to the increased the bulkiness of cation on account of addition of one chlorine atom in the fourth position of the phenyl ring.

An identical structural feature of the two crystallographically independent cations about the $CuCl_4^{2-}$ anion is that their piperazine rings show the usual chair conformation with torsion angles ranging from 55.9° to 63.0°. These values closely resemble those observed in the parent complex [28]. The C-C (1.386Å) and the C-N bond distances 1.4916Å appear to be in good agreement with previous results [29].

The fact that the anisotropic thermal parameters are not very high for Cl and Cu atoms compared to those of other atoms reveals that the $CuCl_4^{2-}$ structure is not disordered or there are no oscillating Cu-Cl bonds. Hence dynamic J-T effect or disorder is ruled out.

Hydrogen bonding interactions

In order to form a square planar geometry, the Cl atoms of $CuCl_4^{2-}$ anion must be engaged in very strong H-bonding which may overcome the Cl-Cl electrostatic repulsion. Further, the crystal field stabilization may also favour square planar geometry in such cases. The trans angle value (166.3°) is slightly lower (by 13.7°) from the ideal trans angle of 180° for the square planar geometry. However, this θ value is far greater than those observed for many tetrachlorocuprates for which the trans angle lies in the range of 132-152°.

The nearly planar $CuCl_4^{2-}$ anionic structure is parallel to the plane bisecting the 'a and 'c axes. Further, the chlorine atoms Cl2, Cl3 and Cl5 have short contacts with C-H bonds of the rings. The three strong H-bonds formed by the two $[4\text{-ClBzPipzH}_2]_2^{2+}$ cations with the $CuCl_4^{2-}$ anion through the N-H bonds leads to a nearly planar arrangement as they link with the lattice Cl^- ions too. Thus an infinite chain along the crystallographic a

axis is formed. The situation is quite similar to the one we encounter in parent complex N-benzylpiperazinium tetrachlorocuprate(II) [28], where the lowest cell dimension is b, whereas for titled crystal it is a. Further, the longest cell dimension is along 'a' axis with a value of 21.954A° and z = 2 whereas in titled compound, the value is nearly double (44.19A°) and z = 4. Hence the chain formation is along the shortest unit cell axis along which the crystal grows faster. The stability of the crystal structure is determined by hydrogen bonding which affects the bond lengths as well as bond angles [29] of the cationic and the anionic units in $[N\text{-}(4\text{-}ClBzPipzH_2]_2{}^{2+}[CuCl_4]^{2-}$.

The effect of molecular association is explained through the extensive hydrogen bonding via hydrogen atoms H2A and H2B, attached to nitrogen atom, N2 of the cationic group in which the Cl3 and Cl5 atoms of $CuCl_4^{2-}$ anion act as acceptor for these N2-H2A.....Cl3 and N2-H2B.....Cl5 hydrogen bonds (table 4, figure 3). Similar results have been reported earlier [30-33]. The network of N-H - - - Cl interactions in which the crystal packing depends is illustrated in figure 3. Further, the free chloride ion of the crystal lattice (Cl2) is also involved in hydrogen bonding network eventhough this atom is far away from the anionic unit. The extensive hydrogen bonding stabilizes the planar geometry with tetragonal distortion in the unequally flattened $CuC1_4^{2-}$ anions, for which no other short interionic contacts were found.

Hydrogen bonding interactions lead to longer Cu-Cl bonds for the Cl atoms involved [34]. The bond distance of Cu-Cl5 (2.321 Å), is the longest among all Cu-Cl distances and is involved in hydrogen bonding with the two neighboring cations. Nevertheless, the Cu-Cl4 has the shortest bond distance of 2.261Å which is not involved in hydrogen bonding. Existence of bifurcated H-bonding is well established between the cations and Cu-Cl5 chlorine atom as portrayed in figure 3 along c-axis. The free Cl2 of anion present in the crystal lattice also exhibits hydrogen bonding interaction with nearest cation.

The crystal structure is stabilized by N-H….Cl hydrogen bonds which link the anions and cations into chains running along the a-axis. The hydrogen bonding interaction is observed in N2-H2A of cation with Cl3 of $CuCl_4^{2-}$ anions. A similar N2–H2A…..Cl3 unit which is symmetry-wise related [-x+2,-y+1,-z] and N–H1 ……Cl2 also show hydrogen bonding interaction with the two Cl^- ions available in the crystal lattice. These two lattice Cl^- ions are separated by normal van der Waals' distance [3.5Å] from Cu bonded Cl atoms. The chlorine atom, Cl1, in the 4-chlorobenzyl piperazine molecule is not involved in the H-bonding. Moreover there is a symmetry transformation #1 –x+2, -y+1, -z and #2 x, -y+3/2, z+1/2 which is used to generate equivalent atom to bring NH_2 moiety of piperazine molecule closer to the free chlorine atom as depicted in the figure 3.

The comparison of the present system with that of reported parent compound implies that the coordination around the metal atom and the crystal packing are similar except for the choice of solvent and bulkiness of cationic group [28].

TGA/DTA analysis

Table 5. Thermal behavior from TGA and DTA analysis

Temperature range °C	Inflexion Point °C	Endo/ exothermic	Experimental weight loss %	calculated %	Assignment
37-202	80		**10**	10.42	2HCl
202-255	208	Endo	---	---	Phase transition
255-350	305	Endo	90	89	Two 4-chlorobenzyl piperazine + metal chloride

Thermal decomposition profile and possible phase transition was determined by TGA and DTA methods. TGA/DTA curves are presented in figure 5 which reveals that there is a massive endothermic decomposition at 305 °C. The decomposition ranges from TG measurements are compiled in table 5 shows a two stage decomposition pattern in the range of 37 °C - 650 °C along with a phase transition. The first step has a base peak at 80 °C showing a weight loss of 10 % for the endothermic decomposition of two HCl molecules probably involving the two lattice Cl^- atoms leaving behind another chlorocuprate without lattice Cl^- ions. The second step has no appreciable weight loss having a base peak at 208 °C. At this temperature, a phase transition occurs. A base peak at 305 °C in the temperature range of 255-350 °C reveals a total mass loss of 89%

associated with the endothermic elimination of one $CuCl_2$ and two 4-ClBzPipz$^+$HCl$^-$ molecules or the entire chlorocuprate(II) [34].

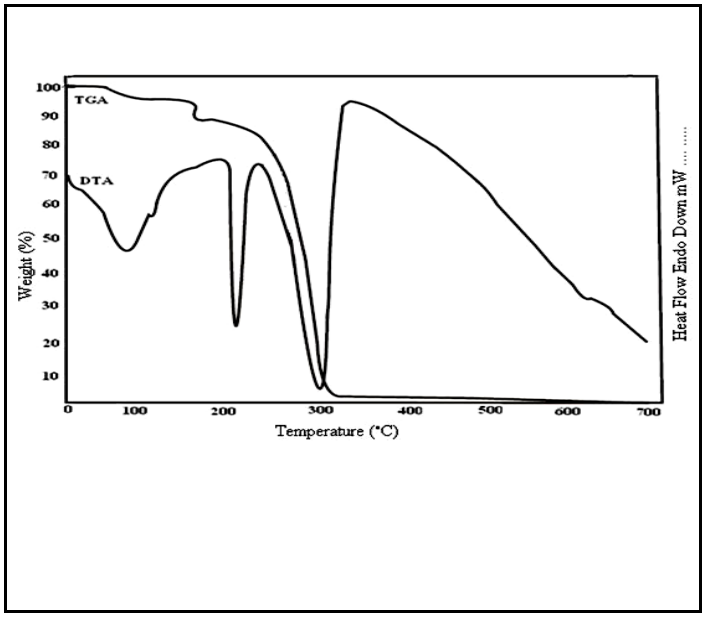

Fig 5. TG and DTA spectrum

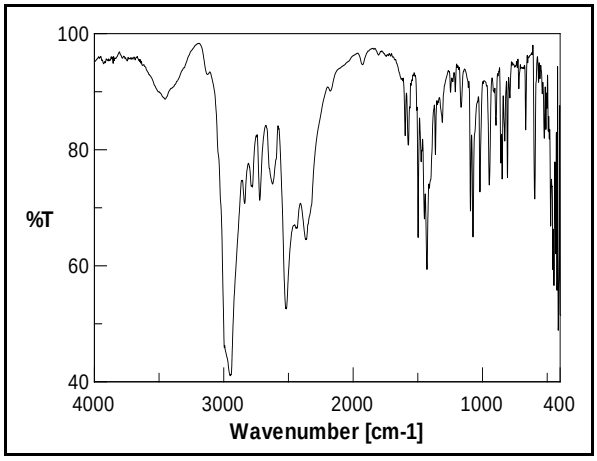

Fig 6. FT-IR Spectrum

FT-IR Spectral analysis

The FT-IR spectrum is presented in figure 6. It reveals the features of organic moiety, N-(4-chlorobenzyl)piperazine only and not that of the tetrachlorocuprate(II). The ν_a(N-H) and ν_s(N-H) stretching frequencies of piperazine moiety, occur at 3406 and 3272 cm^{-1} respectively in free ligand and these values increase to 3460 and 3236 cm^{-1}. This may be due to changes in the hydrogen bonding caused by the presence of $CuCl_4^{2-}$ anions in the lattice. This fact along with the broadening of the peak can be attributed both to the high charge density on the N-H group and the stronger hydrogen bond formation between N-H and Cu-Cl groups as revealed by the crystal structure. Similar effects have been reported earlier [35]. The other peaks correspond to 3123 cm^{-1} (C-H str in aromatic ring); 2950, 2828, 2777 and 2722 cm^{-1} (C-H str in aliphatic group next to nitrogen atom); 1620 cm^{-1} (NH bending of piperazine), 1590 cm^{-1} (C=C str in aromatic), 1455 cm^{-1} (C-C str, aromatic) and 1214 cm^{-1} (C-N str) respectively. The aromatic inplane bending asymmetric vibrational frequency is found to occur at 656 cm^{-1}. The asymmetric and symmetric stretching vibrations of C-C bond occur as a weak band at 1093 and 1073 cm^{-1} respectively.

UV-Visible spectral analysis

The electronic spectrum is presented in figure 7. The peak at 335 nm is assigned to the charge transfer band from the chloride ions to the copper centers within the complex anion. The absorption peak at 450 nm

(22222 cm^{-1}) corresponds to d-d transitions of the Cu^{2+}cation and the band at 320 nm (31250 cm^{-1}) has been tentatively assigned to Cl→ Cu^{2+} charge transfer. The bands at 280 nm and 210 nm (47619 cm^{-1}) respectively may be due to the π-π* electron transition in the organic moiety [36].

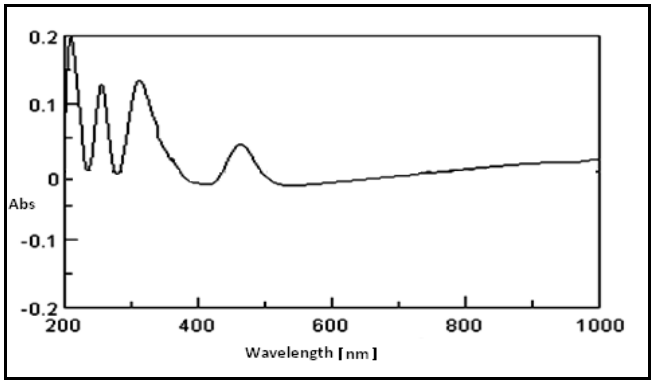

Fig 7. Electronic spectrum

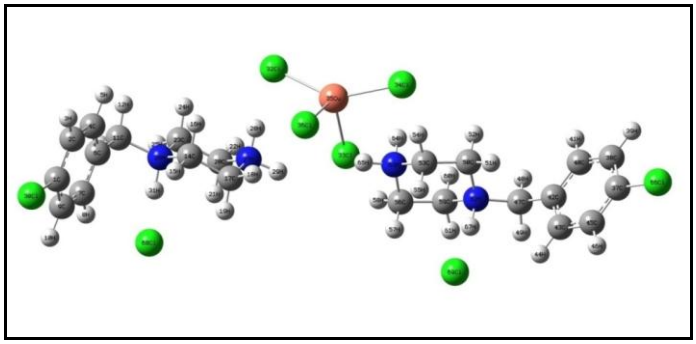

Fig 8. Geometrically Optimized structure

Computational studies: Optimization of the structure

The optimized structure of the complex along with labeling is shown in figure 8. The calculated bond length parameters for unrestricted DFT [37] using the wave function B3LYP [37] employing LANL2DZ basis sets are enumerated in table 2.

A close scrutiny of bond distances (table 2) reveals that the experimental bond length values for the C-Cl linkages in the crystal are 1.732Å and 1.738Å in comparison to the closely occurring calculated values of 1.7550Å and 1.7581Å showing deviations of +0.023Å and +0.0201Å respectively. A similar trend is observed for Cu-N and C-C bonds too with smaller deviations. The other bonds such as C-C and N-C experience larger deviations in the range of 1.373Å to 0.978Å (table 2).

The optimization was carried out with the positional parameters obtained from the the X-ray data as input. The results indicate that the structure expected around $CuCl_4^{2-}$ is closer to a tetrahedral geometry with distortion (θ = 126.27°). However, the experimental data points to a geometry closer to square planar with a small tetrahedral distortion and a flattening angle, θ = 166.305°. This deviation from theoretical prediction indicates that the H-bonding is so effective that the $CuCl_4^{2-}$ anion derives a square planar geometry. This observation is also supported by the H-bonding data (table 4).

HOMO-LUMO energy analysis

The orbital energy level analysis reveals values of +0.003 and -0.003 eV for E_{HOMO} (energy of highest occupied molecular orbital) and E_{LUMO} (energy of lowest unoccupied molecular orbital) respectively. The LUMO is spread largely over the chlorine atom and benzene molecule of cation and to a lesser extent on the other moieties. HOMO appears to disperse all over the anionic sites in the compound. The magnitude of the HOMO-LUMO energy separation is a measure of the reactivity pattern of the molecule [37] and an indicator of the kinetic stability [28, 38]. The compound has a small HOMO-LUMO gap of 0.006eV implying lower kinetic stability and a higher chemical reactivity. The orbital contours of HOMO and that of LUMO of the molecule are shown in figures 9 and 10 respectively.

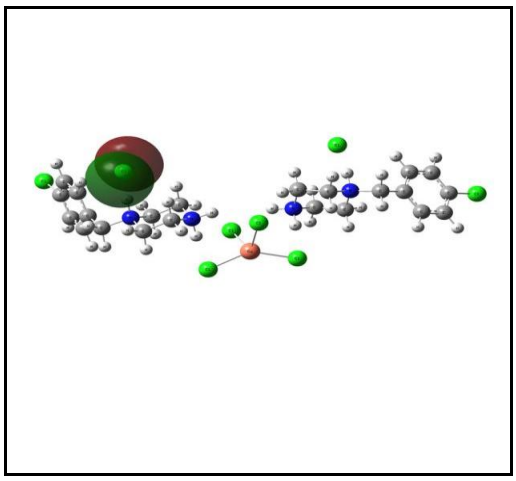

Fig 9. Orbital Contours of HOMO

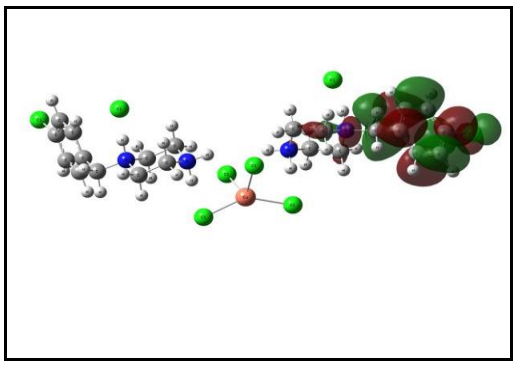

Fig.10. Orbital Contours of LUMO

Charge density

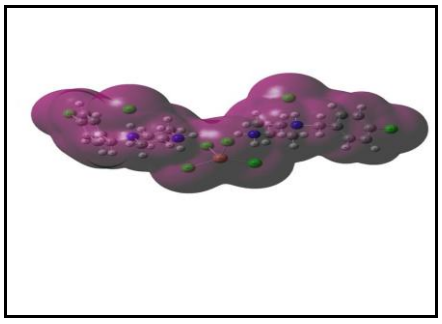

Fig 11. Total charge density distribution

The values of charge density lie in the range of $-6.334e^{-2}$ to $6.334e^{-2}$ which is equally distributed over the entire molecule.

The total electronic charge density calculated for an isolated molecule, $C_{11}H_{17}Cl_4N_2$ is shown in figure 11.

The charge density is distributed such that maximum densities are found in the regions where chlorine and nitrogen atoms are present. It is in accordance with the crystal structure and electro negativity values.

Antimicrobial activity

Antibacterial activity

The lowest concentration (highest dilution) required to arrest the growth of bacteria is regarded as minimum inhibitory concentrations (MIC). Tetracycline was used as the control. The diameter of the zone of inhibition and minimum inhibitory concentration values are given in table 6 which corresponds to values

against *Staphylococcus aureus* as well as *Eschrichia coli* exhibits activity against both the bacteria. Although the activities against both bacteria are comparable, they are greater than the value for the standard drug, tetracycline.

Table 6. The diameter of the zone of inhibition and minimum inhibitory concentration against *Escherichia coli* and *Staphylococcus aureus*

Organism	Inhibition zone (mm)	Control (tetracycline) (mm)
Escherichia coli	2.4±0.42	1.5±5.63
Staphylococcus aureus	2.5±0.39	1.5±4.37

Table 7. Antifungal activity against *Colletotrichum* and *Fusarium* species

Concentration	Zone of inhibition (mm)		Control (tetracycline) (mm)
	Colletotrichum	***Fusarium***	
50 µL/ mL	30	28	60
100 µL/ mL	25	20	50

Antifungal activity

Antifungal activity was revealed by prominent zones observed against fungal plant pathogens of *Colletotrichum* and *Fusarium* species. The zones of fungal growth inhibition against fungal plant pathogens of *Colletotrichum* and *Fusarium* species were determined for two different concentrations (table 7). It is more sensitive at the 100 µL concentration level than at 50 µL range against *Colletotrichum.* However, the order is reversed for *Fusarium* species. It is found that the activities are less than that of the tetracycline standard. The study indicates that the compound has antifungal activity against both fungi employed. The antifungal activity might be due to the presence of heterocyclic amine moiety.

Conclusion

The tetrachlorocuprate(II) anion exhibits an unequally flattened tetrahedron super imposable on to a square planar geometry. It is stabilized by hydrogen bonding network with two largest Cl-Cu-Cl angles being 167.92° and 164.70°. Four independent $(N\text{-}(4\text{-}ClBzPipzH_2)^{2+}$ cations are linked to the anions through their N-bonded hydrogen atoms. The structure was optimized using the positional parameters for all atoms derived from crystal data. The optimized data were employed to arrive at charge density distribution and HOMO-LUMO calculations. The FT-IR study substantiates the H-bonding nature of the cations. X-ray analysis, UV-visible spectral and TGA/DTA analyses reveal the composition and geometry of the tetrachlorocuprate(II) anion as well as the cations.

Appendix A. Supplementary data

CCDC 882861 contain the supplementary crystallographic data for N-(4 chlorobenzyl)piperazinium tetrachlorocuprate(II) complex. The data can be obtained from National Center for Catalysis Research, IITM, Chennai-600036, deposited at the Cambridge Crystallographic Data Centre and allocated the deposition number CCDC 882861 Cambridge Crystallographic Data Centre, 12 Union Road, Cambridge CB2 1EZ, UK; fax: +44 1223 336 033; or e-mail: deposit@ ccdc.cam.ac.uk.

Acknowledgement

The authors thank the management, Thiagarajar College, Madurai-9 and Syngene International Ltd., a Biocon company, Bangalore-99, for permitting N. Dhanam to carry out the research work. We thank National Center for Catalysis Research, Department of Chemistry, IITM, Chennai for solving the crystal structure, providing computational facilities.

References

1. Patrick G.L., An Introduction to Medicinal Chemistry. 2nd edition, Oxford University Press., Mar., 1 (2001).
2. Edwards K., Herringer S.N., Parent A.R., Provost M., Shortsleeves K.C., Turnbull M.M., Dawe L.N., Inorg. Chim.Acta (2011); 368: 141-151.
3. Shin J.Y., Dolphin D., Patrick B.O., Crystal Growth & Design (2004); 4(4): 659-661.
4. Casarin M., Cingolani A., Nicola C. Di., Falcomer D., Monari M., L. Pandolfo, Pettinari C., Crystal Growth & Design (2007); 7(4): 676-685.
5. Adams C.J., Colquhoun H.M., Crawford P.C., Lusi M., Orpen A.G., Angew. Chem. Int. Ed., (2007); 46: 1124.
6. Sang R., Xu L., Inorg. Chem., (2005); 44: 3731-3737.
7. Lee Y.M., Park S.M., Kang S.K., Kim Y.I., Choi S.N., Bull. Kor. Chem. Soc., (2004); 25: 823-828.
8. Lu W.-B, Zhou X.-H, J. Coord. Chem., (2006); 59: 1371.
9. Panja A., Goswami S., Shaikh N., Roy P., Manassero M., Butcher R.J., Banerjee P., Polyhedron (2005); 24: 2921-2932.
10. Lacroix P.G., Clement R., Nakatani K., Zyss J., Ledoux I., Science., (1994); 263: 658-660.
11. Chakravarthy V., Guloy A.M., Chem. Commu., (1997): 697-698.
12. Mitzi D.B., Prog. Inorg. Chem., (1999); 48: 1.
13. Stricker M., Linder T., Oelkers B., Sundermayer J., Green Chem., (2010); 12: 1589-1598.
14. Helmholz L., Kruh R.F., J. Am. Chem.Soc., (1952); 74(5): 1176-1181.
15. Battaglia L.P., BonamartiniCorradi A.B., Marcotrigiano G., Menabue L., Pellacani G.C., Inorg. Chem. (1982); 21(11): 3919-3922.
16. Antolini L., Menabue L., Pellacani G.C., Saladini M., Inorganica Chimica Acta (1982); 58: 193-200.
17. Haddad S., Willett RD., Inorg. Chem., (2001); 40(10): 2457-2460.
18. Kharitonov D.N., Golubeva E.N., Kinetics & Catalysis (2003); 44(4): 513-517.
19. Jotham R.W., Kettle S.F.A., Inorg. Chim.Acta (1971); 5: 183-187.
20. Lohr L.L., Jr., Lipscomb W.N., Inorg. Chem. (1974); 38: 279.
21. Sheldrick G.M., SHELXS97 and SHELXL97, University of Gottingen, Germany, (1997).
22. Becke A.D., J.Chem. Phys. (1993); 98: 5648-5652.
23. Lee C., Yang W., Parr R.G., Phys. Rev. (1988); B37: 785-789.
24. Hay P.J., Wadt W.R., J. Chem. Phys. (1985); 82: 299.
25. Lopez-Gresa M.P., Ortiz R., Perello L., Latorre J., Liu-Gonzalez M., Garcia-Granda S., Perez-Priede M., Canton E., Antibacterial studies J. Inorg. Biochem., (2002); 92: 65.
26. Mark E., Vol'pin E.,, Galina Novodarova N., Nadezhda Yu. Krainova, Lapikova, Vera P., Andrey A., Journal of Inorganic Biochemistry (2000); 81(4): 285-292.
27. K. Robert, Bogges and A. David, J of chemical education (1975) 649.
28. Marzotto A., Clemente D.A., Benetollo F., Valle G., Polyhedron (2001); 20: 171-177.
29. Bhattacharya R., Sinha Ray M., Dey R., Righi L., Bocelli G., Ghosh A., Polyhedron (2002); 21(25): 2561-25-65.
30. Harlow R.L., Wells W.J., Watt G.W., Simonsen S.H., Inorg. Chem., (1975); 14: 1768.
31. Golubeva E.N., Kharitonov D.N., Kochubey D.I., Ikorskii V.N., Kriventsov V.V., Kokorin A.I., Sotetsner J., Bahnemann D.W., J. Phys. Chem., (2009); A 113: 10219--10223.
32. Halvorson K.E., Patterson C., Willett R.D., Acta Cryst., (1990); B 46: 508.
33. Byrappa K., Kandhaswamy M.A., Srinivasan V., Cryst. Res. Technol., (1999); 34: 843.
34. Clemente D.A., Marzotto A., Valle G., Visona C.J., Polyhedron (1999); 18: 2749-2757.
35. V. Chakravarthy, A. M. Guloy, *Chem. Communication* (1997) 697.
36. Frisch M.J., Gaussian03, Revision-D., (2004); 01.
37. Textor M., Dubler E., Oswald H.R, Inorg Chem., (1974); 13: 1361.

*****